JOURNAL OF GEOPHYSICAL RESEARCH, VOL. 97, NO. D15, PAGES 16,511–16,522, OCTOBER 30, 1992

Atmospheric Measurements of Peroxyacetyl Nitrate and other Organic Nitrates at High Latitudes: Possible Sources and Sinks

H. B. SINGH,[1] D. O'HARA,[2] D. HERLTH,[1] J. D. BRADSHAW,[3]
S. T. SANDHOLM,[3] G. L. GREGORY,[4] G. W. SACHSE,[4] D. R. BLAKE,[5] P. J. CRUTZEN,[6] M. A. KANAKIDOU[6]

Aircraft measurements of peroxyacetyl nitrate (PAN) and other important reactive nitrogen species (NO, NO_2, HNO_3, peroxypropionyl nitrate (PPN), CH_3ONO_2, NO_y) were performed at high latitudes over North America and Greenland during July-August 1988, at all altitudes between 0 and 6 km as part of an Arctic Boundary Layer Expedition (ABLE 3A). Complementing these were measurements of C_1 to C_5 hydrocarbons, O_3, chemical tracers (C_2Cl_4, CO), and important meteorological parameters. PAN was found to be an important reactive nitrogen species in the free troposphere, with 95% of the mixing ratios falling in the range of 5 to 450 ppt. PAN increased systematically with height with mixing ratios of 100-700 ppt at 6 km and 0-50 ppt in the boundary layer. The free tropospheric PAN reservoir was present over the entire high-latitude region sampled (50° to 82°N latitude and 60° to 160°W longitude). In the boundary layer, PAN mixing ratios were higher over land than over the North Pacific Ocean. Significant levels of PAN were measured within stratospheric intrusions, forest fire plumes, and episodes of remote pollution. Other organic nitrates such as PPN and CH_3ONO_2 were found to be a small fraction of PAN (0-10%). PAN and O_3 were strongly correlated both in their fine and gross structures, and the latitudinal distribution of PAN in the free troposphere followed that of O_3. A two dimensional global photochemical model is used to compare measurements and model results. Model simulations, correlations between reactive nitrogen species (e.g. PAN and NO_y) and anthropogenic tracers (C_2H_2, CO, C_2Cl_4), and the composition of NO_y itself support the view that the reactive nitrogen measured during ABLE 3A is predominantly of anthropogenic origin with a minor stratospheric component. Transported industrial pollution, biomass burning, and the unique seasonal dynamics of the Arctic/sub-Arctic region play a dominant role in defining this reactive nitrogen abundance. This PAN (and NO_y) reservoir may contribute to the summertime maximum in deposited nitrate observed over Greenland.

INTRODUCTION

A long–term goal of the NASA Global Tropospheric Experiment (GTE) is to understand the atmospheric chemistry associated with Earth's major ecosystems [*McNeal et al*, 1983]. The Arctic Boundary Layer Expedition (ABLE 3A) is a component part of GTE and was conceived to study the high–latitude (Arctic/sub–Arctic) environment of the northern hemisphere. It is now generally believed that despite the remoteness of the arctic atmosphere, significant human influences are beginning to impact this region especially in winter and early spring [*Schnell*, 1984; *Rahn*, 1985; *Barrie*, 1986]. Another reason for investigating the Arctic/sub–Arctic environment is the high predicted sensitivity of this region to climatic change resulting from human activities and the extreme paucity of available data from these regions. This aircraft and ground study, performed in the summer of 1988 (July–August), sought to investigate atmospheric photo–chemical and transport processes associated with the high latitude atmospheric system. An overview of the ABLE 3A field study has been provided by *Harriss et al.* [this issue].

It is well known that reactive nitrogen plays a central role in the chemistry of the atmosphere [*Haagen-Smit*, 1952; *Levy*, 1971; *Logan et al.*, 1981]. The high–latitude environment has been insufficiently studied, and much of the available information is from the winter/spring Arctic haze period [*Schnell*, 1984; *Rahn*, 1985]. It is generally believed that summertime Arctic atmosphere is extremely clean [*Barrie*, 1986]. Although a body of data on organic nitrogen species has become available in recent years, very little of it is relevant to the free tropospheric environments of the high latitudes [*Singh et al.*, 1986, 1990*a*, *b*; *Rudolph et al.*, 1987; *Bottenheim and Gallant*, 1989] . ABLE 3A provided a unique opportunity to measure a large number of reactive nitrogen species (NO, NO_2, $CH_3C(O)OONO_2$ peroxyacetyl nitrate, or (PAN), $C_2H_5C(O)OONO_2$ peroxypropionyl nitrate, or (PPN), CH_3ONO_2, HNO_3, and NO_y (total odd nitrogen) to an altitude of 6 km during the summer (July–August) of 1988. A comprehensive set of related chemical [O_3, C_2–C_5, NMHC (nonmethane hydrocarbons), CO, C_2Cl_4] and meteorological parameters were also measured. In this paper we describe the measurements of PAN and other reactive nitrogen species during ABLE 3A and use the transit flights to characterize their north-south and east-west gradients in the free troposphere. Relationships between the atmospheric concentrations of PAN and other key chemical parameters (such as NO_x, NO_y and O_3) are explored to assess the sources and sinks of PAN and NO_y.

EXPERIMENTAL

ABLE 3A utilized a Lockheed Electra for all aircraft measurements. Instrument integration and flight tests were performed at Wallops Island, Virginia. A total of 33 missions, including transit flights, were performed from July 7 to August 17, 1988. Aircraft missions were conducted from Barrow, Alaska (missions 6–13; July 12 to 24), Bethel/Cold Bay, Alaska (missions 14–26; July 26 to August 10), and Thule, Greenland (mission 29; August 13). The remainder were transit flights. A typical flight mission lasted approximately 5 hours.

[1]NASA Ames Research Center, Moffett Field, California.
[2]San Jose State University Foundation, Moffett Field, California.
[3]Georgia Institute of Technology, Atlanta.
[4]NASA Langley Research Center, Hampton, Virginia.
[5]University of California, Irvine.
[6]Max-Planck Institut für Chemie, Mainz, Germany.

Paper number 91JD00889
0148-0227/92/91JD-00889$05.00

Flight missions during ABLE 3A were divided into generic types that included boundary layer flux measurements, mid-tropospheric distributions and vertical profiles. Geographical extent covered during the ABLE 3A missions and a summary table of individual flights is provided in the overview paper by *Harriss et al.* [this issue].

PAN was measured by an electron-capture gas-chromatographic technique. Along with PAN, it was also possible to simultaneously obtain a PPN, CH_3ONO_2 and C_2Cl_4 measurement when detectable levels (1 to 5 ppt) were present. Typically, 100 to 200 mL of ambient air were pre-concentrated at a controlled -150°C temperature. PAN calibrations were performed by using a diffusion tube filled with liquid PAN in a *n*-tridecane matrix. For routine calibrations a diffusion tube (5 mm ID) was filled and held at ice-water temperature in a specially constructed dewar. Air flowed over this tube at a known rate. The PAN in the exit stream was measured by using an NO_y detector. A nylon filter was inserted in line to remove any traces of nitric acid. A small correction (3 to 7%) was applied to account for trace quantities of methyl nitrate that were nearly always present. A two-step dynamic dilution system was used to generate low-ppt mixing ratios of PAN. A measurement sensitivity of better than 5 ppt PAN was achievable with a 100-mL air sample. Instrument precision and accuracy are estimated to be ±10% and ±25%, respectively. Additional details of this and similar techniques can be found elsewhere [*Singh and Salas*, 1983, *Joos et al.*, 1986; *Fehsenfeld et al.*, 1987; *Singh et al.*, 1990*a*]. Methyl nitrate mixing ratios were calculated by using gas phase coulometery [*Lillian and Singh*, 1974]. Preliminary tests suggest that this should be accurate to ±50%. Nitric acid was measured by the mist chamber technique developed by *Talbot et al.* [this issue]. NO, NO_2, and NO_y were measured by a laser-induced fluorescence (LIF) technique described by Sandholm et al. [this issue].

Results and Discussion

This paper presents an analysis of the distribution and variability of PAN (also PPN and CH_3ONO_2) and its relationships with measured chemical and meteorological parameters for the high-latitude troposphere. A companion paper discusses the partitioning between active and total odd nitrogen [*Singh et al.*, this issue]. Meteorological analyses involving synoptic conditions and 72-hour isentropic back trajectories are provided by *Shipham and Bachmeier* [this issue] and *Drewery* [1988]. Flights deployed from Barrow (71°N) and Bethel (61°N) are used to describe the "Arctic" (missions 6–13) and "sub-Arctic" (missions 14–26) distributions, respectively. The term "all data" is used for all flights north of 50°N (missions 2–32). Twelve transit flights (missions 1–5 and 27–33) provided opportunities for maximum latitudinal and longitudinal coverage. In this and the companion paper [*Singh et al.*, this issue], latitudinal variations from 35° to 82°N are described based on transit missions 1–3 (July 7 to 8) and 29–33 (August 13 to 17). Longitudinal coverage (60° to 160°W) for the high-altitude environment (65° to 80°N) is described based on missions 4 (July 9) and 28 (August 12). Data in such instances are typically combined from altitude bands of 4 to 5.5 km. During the deployment there were also opportunities to sample plumes of air involving pollution episodes, forest fires, and stratospheric intrusions.

Some data selection procedures were necessary, since species were measured by multiple investigators, and sampling times often did not overlap. NO_x data were generally available from direct measurements of NO and NO_2. In some instances where only NO data were reported, NO_x was calculated by utilizing interpolations of the NO_x to NO ratio. For the purposes of this and the companion paper all data were made to conform with the PAN sampling period. When sampling times did not exactly overlap, a linear interpolation was employed. This selection scheme led to a reasonable description of the original data, except in the case of HNO_3. To accommodate the extremely long sampling time for HNO_3, all other data were reduced to conform with this rather coarse time resolution. This file was used in all instances involving HNO_3 data. Model simulations are performed with a two dimensional global photochemical model described in *Kanakidou et al.* [1991].

Mixing Ratios, Variabilities, and Vertical Structures

PAN. Figure 1*a* shows the mean, minimum, and maximum mixing ratios of PAN measured during each of the ABLE 3A

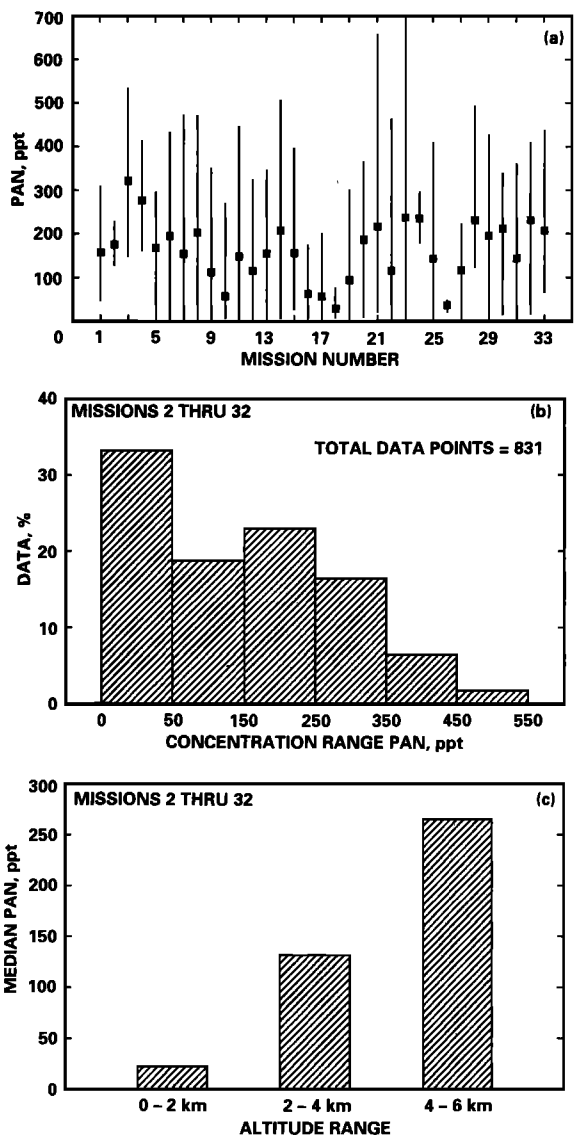

Fig. 1. PAN mixing ratios during ABLE 3A. Solid squares (*a*) show mean PAN mixing ratios (ppt = 10^{-12} v/v) for each mission. Vertical lines indicate maximum and minimum measured values. (*b*) Frequency distribution of PAN mixing ratios over high latitudes (missions 2–32). (*c*) Median PAN mixing ratios in 2-km altitude bands.

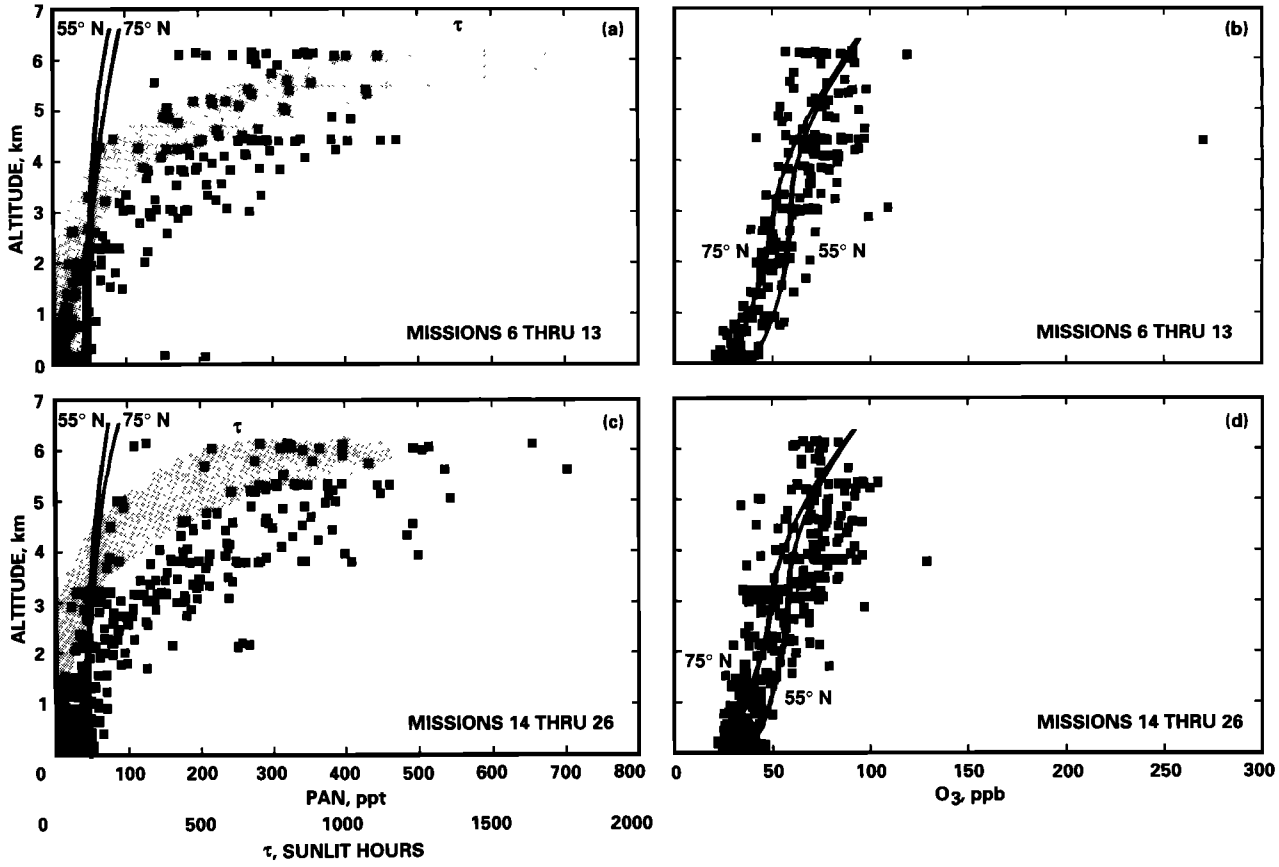

Fig. 2. Vertical distribution of PAN and O_3 in the high-latitude troposphere. Arctic and sub-Arctic data based on flights deployed from (*a*, *b*) Barrow (71°N), and (*c*, *d*) Bethel, (61°N) Alaska. Shaded area indicates computed PAN lifetime (τ) as defined in (1). Dark lines for 55°N and 75°N are calculated from the ethane/propane 2-D model of *Kanakidou et al.* [1991].

missions. The mean mixing ratios were typically in the 100-200 ppt range. Ninety percent of the measurements fell in a range of 0 to 350 ppt (Figure 1*b*) with a maximum value of 700 ppt. Mixing ratios of PAN, expressed in median values, increased with altitudes (Figure 1*c*). The vertical structure of PAN and O_3 for the Arctic and sub-Arctic region is shown in Figure 2. A superposition of PAN data from Barrow (Figure 2*a*) and Bethel (Figure 2*c*) shows that the vertical structures are nearly identical, supporting the conclusion that the high-latitude PAN reservoir is a large-scale phenomenon. It is further noted that the corresponding O_3 structures (Figures 2*b* and 2*d*) over these two high-latitude regions are also very nearly identical. Overall, although PAN vertical profile is much steeper than that of O_3, both species increase rapidly with height between 50° and 75°N latitudes.

The low PAN concentrations in the boundary layer are probably associated with its rapid thermal dissociation rate at warmer surface temperature. The lifetime of PAN (τ) can be defined by (1) [*Singh*, 1987]:

$$\tau=\{1+0.43[NO_2/NO]\}/\{k_1+k_2[OH]+0.43k_2[OH][NO_2/NO]\} \quad (1)$$

where $k_1=1.12 \times 10^{16} \exp(-13{,}330/T)$ s^{-1} and $k_2=1.23 \times 10^{-12} \exp(-651/T)$ cm^3 $molecule^{-1}s^{-1}$.

Rate constants k_1 and k_2 are due to PAN thermal decomposition and reaction with OH, respectively. PAN lifetime in sunlit hours (τ) from the above expression was derived by using temperature T and $[NO_2/NO]$ ratio determined from direct measurements. July mean OH values as computed by *Kanakidou et al.* [1991] were employed. At 55°N, OH values were 2.1 x 10^6 molecule cm^{-3} and 1.7 x 10^6 molecule cm^{-3} for 0.3-km and 5.6 km altitudes, respectively. Mean temperatures during ABLE 3A were 282(±10)°K near the surface and decreased nearly linearly to 250(±7)°K at 6 km. It is evident from (1), that τ is a strong function of temperature. Superimposed on the vertical profile of PAN is the computed value of its lifetime (Figures 2*a* and 2*c*). Although mixing processes modify the vertical profile of a trace gas, it is likely that the thermal dissociation of PAN is a major factor in defining its vertical structure. It is noted that the PAN lifetime at 6-km altitude is nearly a month compared to a few hours in the boundary layer. Hence a vertical structure such as the one observed is relatively easily established, provided a persistent source of PAN is available.

While there are good reasons for both PAN and O_3 mixing ratios to increase with height due to their increasing lifetime and the stratospheric source, respectively, such features were also found for a variety of other trace chemicals throughout the ABLE 3A program. Figure 3 shows an example of the vertical structure of C_2H_2, CO, C_2H_6, and C_2Cl_4 as measured over Barrow. In many instances the hydrocarbon vertical profile shows higher concentrations aloft in a pronounced manner as shown by *Blake et al.* [this issue]. All these species are of terrestrial origin with a significant anthropogenic component. A possible explanation for such a vertical structure is that industrial pollution is transported to this region from the industrial centers of the northern hemisphere via upper

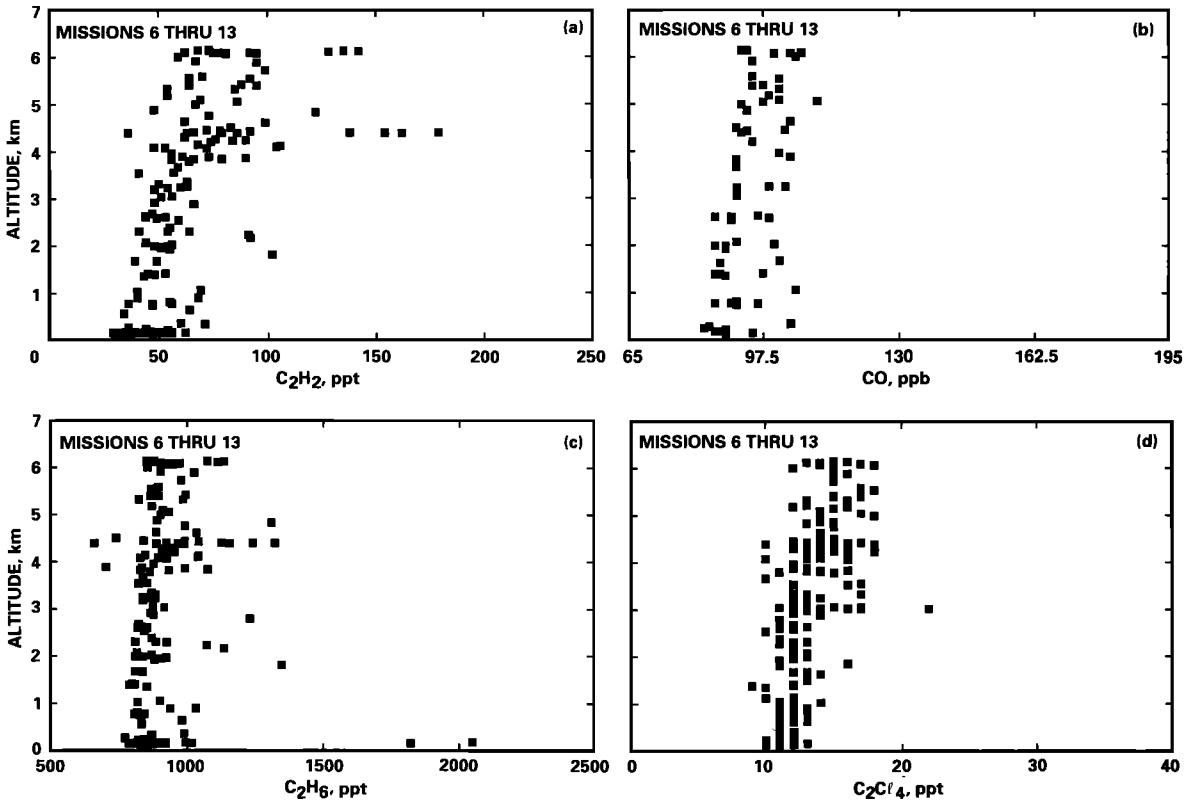

Fig. 3. Vertical distribution of select tracer molecules in the Arctic based on flights deployed from Barrow (missions 6-13).

tropospheric circulation. Superimposed on this are intrusions from the stratosphere and forest fire plumes. As we shall see later, the nitrogen and possibly O_3 chemistry of the Arctic is strongly affected by anthropogenic influences.

What is the possible source of this PAN (and NO_y) reservoir? A persistent source of PAN must come from either direct transport of PAN or NMHC/NO_x photochemistry associated with the high-latitude environment. The primary emissions of NO_x in the high-latitude region are small because of low population density, negligible soil fluxes ($\approx 2 \times 10^8$ molecules. cm^{-2} s^{-1}), and an extremely small lightning and stratospheric source [Bakwin et al., this issue; Isaksen and Hov, 1987]. Three-dimensional (3-D) models of the global troposphere show only a small amount of NO_y coming from the stratosphere (10–80 ppt at 5.5 km and <1 ppt near the surface) and essentially all of it is in the form of HNO_3 [Levy et al., 1980; Kasibhatla et al., 1991], (J. Penner, private communication, 1991). Thus stratosphere is not likely to be a major source of PAN or NO_y. Also, as we shall see late, PAN mixing ratios behave in a manner that is similar to those of a variety of anthropogenic tracers. A conceptual model that is consistent with the available information is that high levels of pollution transported from industrial regions, with significant NMHC and NO_x loading, are trapped in the stable Arctic atmosphere in winter and early spring ("arctic haze") and this charged reservoir photochemically generates significant quantities of PAN (and O_3) as sunlight and summer approach. Natural forest fire plumes also intermittently impact this region [Wofsy et al., this issue]. Measurements from Barrow (71°N) and Spitzbergen (76°–80°N) clearly show that high concentrations of C_2-C_6 NMHC (reactive alkenes, alkanes, and aromatics) are present in the springtime and are drastically lower in summer [Rasmussen et al., 1983; Hov et al., 1984]. Although no multiseasonal reactive nitrogen measurements were performed by these investigators, it is reasonable to assume that large amounts of NO_y coexisted with these NMHC. Limited ground level PAN measurements by Penkett and Brice,[1986] and NO_y measurements by Honrath and Jaffe (The seasonal cycle of nitrogen oxides in the arctic troposphere at Barrow, Alaska, submitted to *Journal of Geophysical Research*, 1992) are also consistent with this conceptualized view.

Most 3-D models of the troposphere do not incorporate any PAN chemistry and incorrectly assume that the bulk of NO_y is HNO_3 [*Levy and Moxim*, 1989; *Penner et al.*, 1990]. A 2-D model of the troposphere with PAN synthesized from background levels of ethane and propane and a total NO_x source of 38 Tg/yr (industrial emissions 20 Tg/yr; soil emissions 6 Tg/yr, biomass burning 6 Tg/yr, lightning 5 Tg/yr, stratosphere 1 Tg/yr) was used to simulate the reactive nitrogen chemistry of the troposphere [*Kanakidou et al.*, 1991]. This model was unable to reproduce the large PAN mixing ratios observed during ABLE 3A (dark lines in Figures 2*a* and c), although O_3 vertical structures could be simulated. Such a model is inadequate to simulate the complex dynamics associated with the Arctic region over a 6– to 9–month period. The results further suggest that a far more complex array of NMHC are involved in PAN synthesis than are present in this model. A reasonable model simulation of O_3, with a significant stratospheric source, and a major under-prediction of PAN (and NO_y) further suggest that the stratosphere is not likely to be a major source of the observed NO_y. It is pertinent to note that the composition of this NO_y [*Singh et al.*, this issue; *Sandholm et al.*, this issue] is substantially different from that of the high-latitude lower stratosphere, which is

principally made up of HNO_3 [*Hübler et al.*, 1990; *Kondo et al.*, 1990].

Davidson et al. [1989], based on sampling from snowpits at 2.6-km elevation, report a distinct summertime maximum in deposited nitrate over Greenland. During this time the airborne nitrate concentration at the three Canadian Arctic surface sites is nearly at a minimum. Measurements made during ABLE 3A clearly show that elevated sites can be exposed to a much higher concentration of reactive nitrogen. Direct deposition of PAN and other NO_y species, along with their oxidation products (PAN $\rightarrow$ NO_2 $\rightarrow$ nitrate), and organic nitrate reservoir and their dry deposition could contribute in an important fashion to the observed summertime maximum in deposited nitrate in the Greenland snowpits.

PPN and CH_3ONO_2. PPN mixing ratios were extremely low and were typically only 5–10% of PAN. Given the PPN detection sensitivity of about 5 ppt, it could only be measured when PAN mixing ratios were 100 ppt or larger which was often the case only in the free troposphere. While the overall PPN structure is expected to be similar to PAN [*Kasting and Singh*, 1986; *Kanakidou et al.*, 1991], its mixing ratios are only a small fraction of the available reactive nitrogen. Figure 4*a* shows the distribution of measured data with levels of 5–20 ppt in the upper troposphere.

The mixing ratios of CH_3ONO_2 were even smaller than those of PPN. It could often be measured only because of its nearly fourfold superior detection sensitivity compared to PPN. The distribution of CH_3ONO_2 was inverted compared to PAN and PPN, with highest mixing ratios in the boundary layer. Figure 4*b* shows its vertical distribution based on measured values only. Despite the preliminary nature of these data, it is evident that CH_3ONO_2 is probably not a significant component of the Arctic reactive nitrogen budget. The main source of this CH_3ONO_2 is likely to be from PAN decomposition ($CH_3COOONO_2$ $\rightarrow$ CH_3ONO_2+CO2). Unlike CH_3ONO_2, however, higher alkyl nitrates (>C_2) are favorably synthesized from the oxidation of higher hydrocarbons (RO_2+NO $\rightarrow$ $RONO_2$) and may exist in significant quantities. Because of the fundamentally different mechanism for CH_3ONO_2 and $RONO_2$ synthesis, the near absence of CH_3ONO_2 in no way implies that other alkyl nitrates are also absent. It is worth noting however, that the higher alkyl nitrates are somewhat more reactive and may be removed at a faster rate [*Atkinson*, 1990]. If the conceptualized mechanism for arctic PAN and NO_y is correct, then significant quantities of simple and multifunctional organic nitrates must surely be present [*Calvert and Madronich*, 1987; *Singh*, 1987].

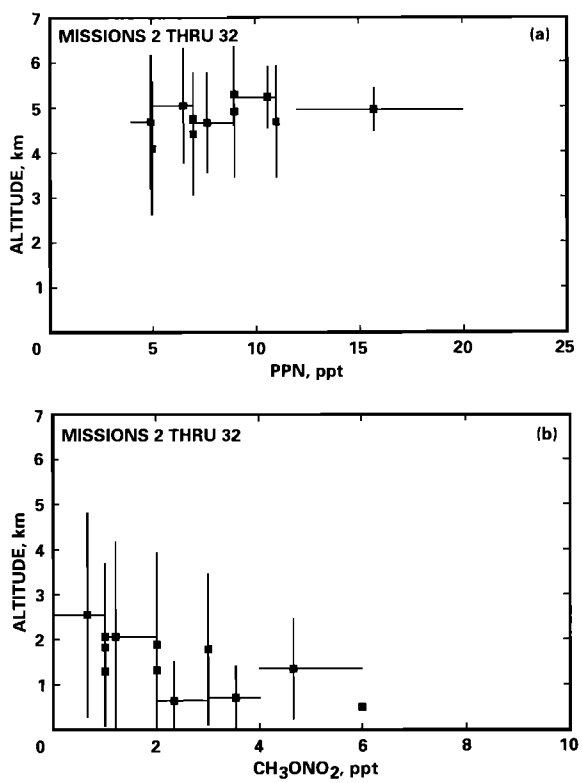

Fig. 4. Peroxypropionyl nitrate (PPN) and methyl nitrate in the high-latitude troposphere (>50°N). Each solid square represents a mean of 15 consecutive data points. Vertical lines show ±1σ. Horizontal lines indicate the maximum and minimum mixing ratio for the binned data (15 data points). In all subsequent figures, binned data are described in this manner only.

Latitudinal and Longitudinal Variations

As stated earlier, it was possible to arrange transit flights during outbound (missions 1 to 4) and inbound (missions 28-33) journeys in such a way as to gain maximum latitudinal (35° to 84°N) and longitudinal (60° to 160°W) coverage. These transit flights provided extensive opportunities for sampling in the free troposphere at around 5-km altitude.

Latitudinal profiles. The free tropospheric latitudinal profile of PAN during outbound (missions 1–3) and return (missions 29 to 33) transit flights is shown in Figure 5. Since PAN is not a conserved species, corresponding O_3, NO_x, and NO_y mixing ratios are also shown. It is noted that north of 45°N, the mean temperature of the sampled air during missions 1–3 was 5° to 10°K warmer than that of missions 29–33. This is a result of both altitude variations and different synoptic meteorology. Figures 5*a* and 5*c* clearly show that PAN levels in the vicinity of 100 to 400 ppt were present in the free troposphere between 35° and 85°N latitudes. PAN concentrations are higher at northern latitudes only during the outbound flights (Figure 5*a*), but no such systematic gradient was observed during the inbound flights (Figure 5*c*). In both instances, a great deal of variability is present. PAN structure over the entire latitudinal belt is nearly coincident with the corresponding O_3 structure. Similar types of PAN-O_3 latitudinal behavior have been reported by *Singh et al.* [1990*b*] from lower latitudes (35°N to 0°N) in the northern hemisphere. It is becoming evident that atmospheric phenomena that define PAN distribution also define the corresponding O_3 behavior. It is also noted that while the NO_x latitudinal profile consistently showed higher values at lower latitudes (Figures 5*b* and 5*d*), possibly because of proximity to sources, such was not the case for NO_y. NO_y, a more conserved quantity, showed only a small latitudinal gradient even though the NO_y levels during missions 1–3 were nearly double those encountered during missions 29–33 (Figures 5*b* and 5*d*).

Also shown in Figure 5 (dashed line) is the systematic PAN, NO_x, and NO_y latitudinal trend predicted by the ethane/propane model (5.6-km level) of *Kanakidou et al.* [1991]. As is discussed in the companion paper [*Singh et al.*, this issue], NO_x is roughly in equilibrium with PAN and under-prediction of PAN also ensures the same for NO_x. The model, probably because of its inability to simulate complex Arctic/sub-Arctic dynamics, also significantly under-predicts NO_y.

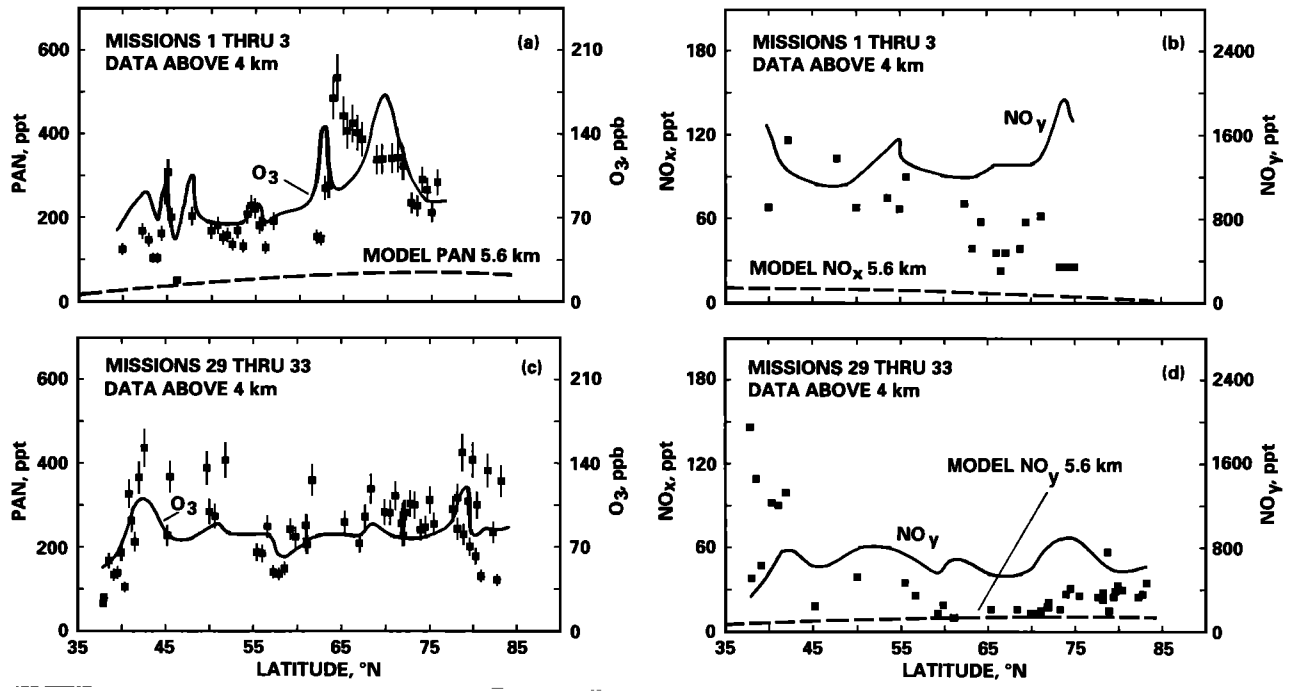

Fig. 5. Latitudinal distribution of PAN as measured during outbound (missions 1 to 3) and inbound (missions 29 to 33) ABLE 3A transit flights. (*a*, *c* Superimposed on PAN data is the corresponding O_3 profile shown by the dark line. (*b*, *d*) NO_x and NO_y data are shown for comparison. All data are from 4 to 5.5-km altitude band. Mean temperatures during missions 1-3 were about 5°C warmer than missions 29-33. Dashed line is calculated for 5.6-km altitude from the ethane/propane 2-D model of *Kanakidou et al.* [1991].

Figure 6 shows similar latitudinal profiles of tracer molecules. In almost all these instances, species are more abundant at higher latitudes. However, air masses in the free troposphere appear to be relatively well mixed north of the typical summer jet stream position at 50°N. This is consistent with the distribution of NO_y, and implies that free tropospheric circulation, at least in the summer, results in rather rapid mixing between high and mid-latitudes. Overall, it appears that the Arctic is somewhat polluted in summer but a significant fraction of NO_x has been oxidized to reservoir species.

Longitudinal profiles. PAN mixing ratios show no systematic trend as a function of longitude (Figure 7). Substantial variability throughout this latitude belt (65° to

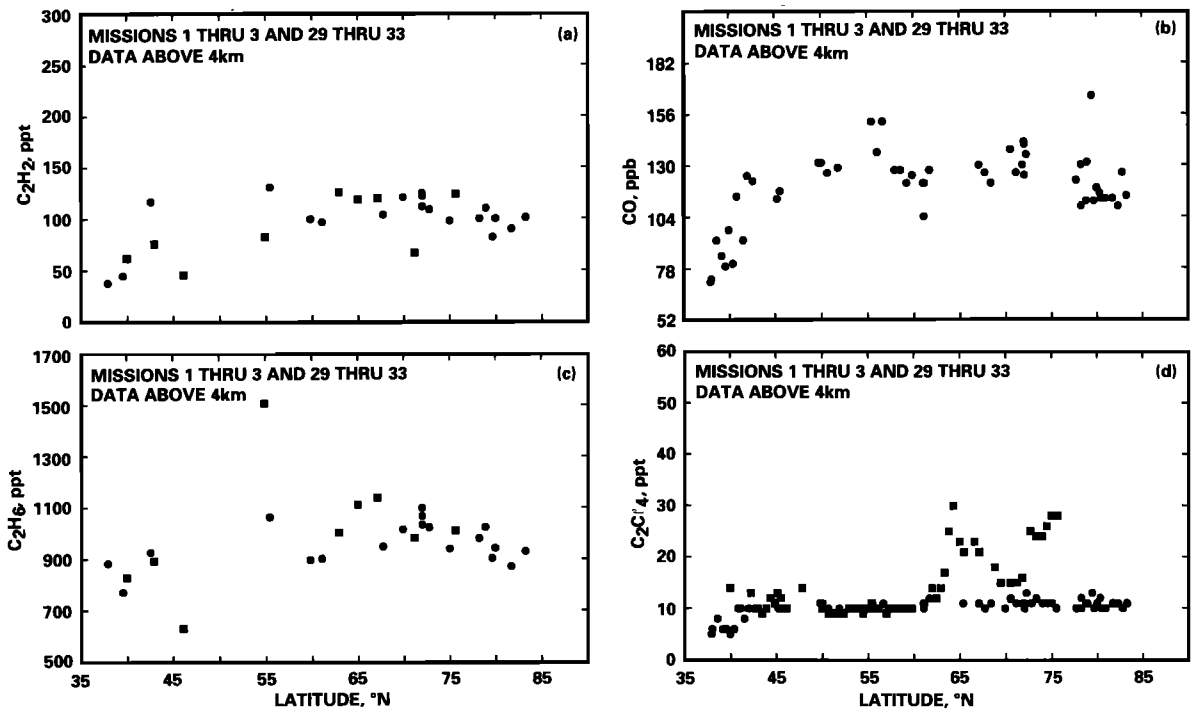

Fig. 6. Latitudinal distribution of select tracer molecules based on outbound (missions 1-3) and inbound (missions 29-33) ABLE 3A flights. Dark squares and circles represent data from missions 1-3 and 29-33 respectively. As in Figure 5.

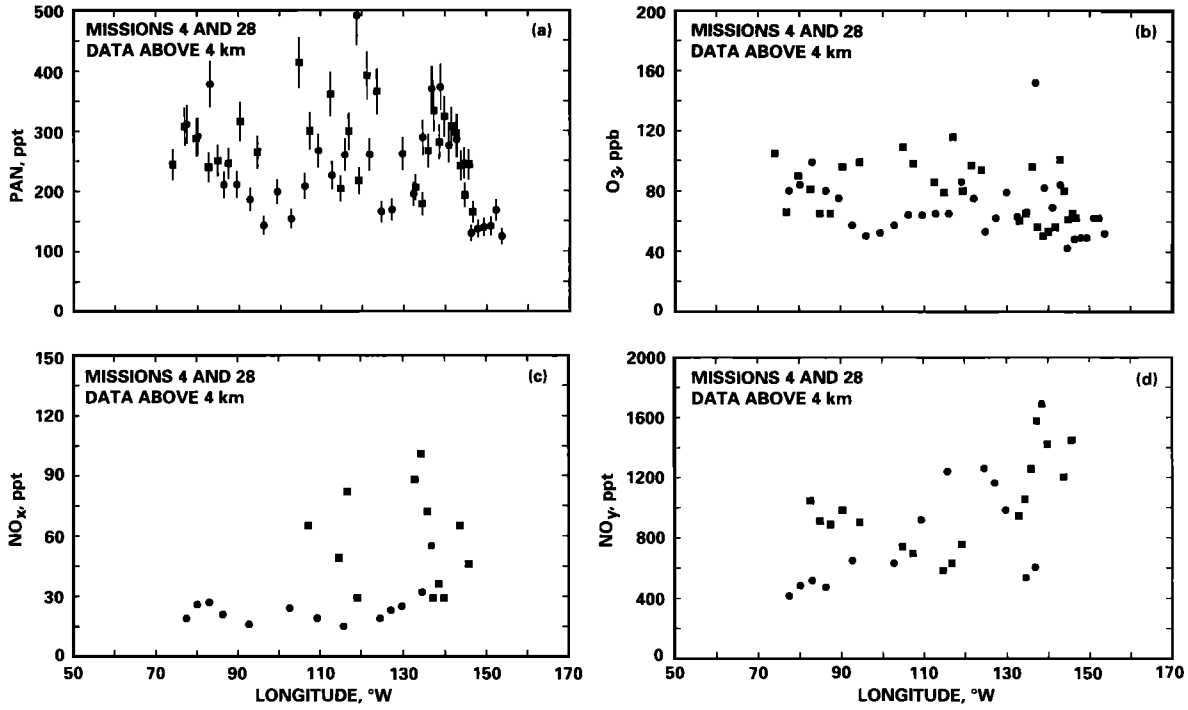

Fig. 7. Longitudinal distribution of PAN in the high latitude (65° to 80°N) free troposphere. (*b–d*) Corresponding O_3, NO_x and NO_y data are shown for comparison. Dark squares represent data from mission 4, and dark circles from mission 28. Mission 4 data (65° to 77°N) are from an altitude band of 4.8 to 6.1 km and mission 28 data (70° to 80°N) are from a somewhat lower 4.5– to 5.2-km altitude band.

80°N) is observed both in PAN and O_3 abundances. It is noted, however, that a part of this variability is due to altitude dissimilarities. For example, mission 4 (solid squares) data are for an altitude band of 4.8 to 6.1 km, while mission 28 (solid circles) data are from a lower altitude band of 4.5 to 5.2 km. Figure 7*a* clearly shows that the high-latitude PAN reservoir is a large-scale phenomenon that extends from 60° to 160°W longitudes and probably beyond. These and the previously published results [*Singh et al.*, 1990*a*, *b*] leave little doubt that a hemispheric-scale reservoir of PAN is present in the upper troposphere.

Relationships With Chemical Parameters

Ozone. As stated earlier, PAN and O_3 showed similar latitudinal and vertical behavior. Figure 8 shows significant PAN-O_3 correlations for the entire high-latitude data set as well as for the Arctic and sub-Arctic subsets. Such correlations have also been previously reported from mid-latitudes and the tropics [*Singh et al.*, 1990*a*, *b*]. These correlations are suggestive of a common source of PAN and O_3. The photochemical oxidation of continental NMHC (natural and anthropogenic) and NO_x precursors, is most likely responsible. The additional possibility that the large-scale atmospheric structures of PAN and O_3 are similar (both increase with altitude), and the observed correlations are largely due to dynamical processes also needs to be investigated. It is highly unlikely that the stratosphere is a cause of these correlations as high PAN values are not expected there.

To investigate the reasons for these correlations we performed limited studies with the 2-D photochemical model of *Kanakidou et al.* [1991]. In this 2-D model, nearly all of O_3 resulted from stratospheric injections and $CH_4/CO/NO_x$ chemistry, while PAN was synthesized exclusively from $C_2H_6/C_3H_8/NO_x$ chemistry. The model-predicted PAN mixing ratios were much lower than those measured. However, because of the fairly detailed simulation of PAN and O_3 chemistry, it was felt that the model may still capture the mean PAN and O_3 atmospheric structures. It was possible to generate some similarities in the mean vertical structures of PAN and O_3 at high latitudes [*Kanakidou et al.*, 1991]. No such similarities could be calculated for middle or low latitudes. The reasons for the similarities in the large-scale structures are complex but probably are related to the common NO_x needed for both PAN and O_3 synthesis, as well as some coincidental similarities in sources and sinks. For example, PAN may be high in the upper troposphere because of its thermal stability (long lifetime), while O_3 may be high because of its stratospheric source. Similarly, PAN may be low in the lower troposphere because of its fast thermal dissociation (short lifetime), while O_3 may be low because of surface deposition and, in the marine boundary layer, net photochemical O_3 destruction due to insufficient NO_x.

It would seem that an important reason for PAN-O_3 correlations is due to the impact of continental precursors on the Arctic/sub-Arctic photochemistry. However, dynamically generated correlations due to similar mean vertical structures of PAN and O_3 probably also play a role. Advanced 3-D models of the troposphere and more atmospheric data on PAN, O_3, and precursors are required to fully understand the reasons for the observed correlations.

NO_x. NO_x is both a necessary precursor as well as a product of PAN. Figure 9 shows the PAN-NO_x relationships for the high latitudes. PAN increases with increasing NO_x for NO_x values up to about 60 ppt. At higher NO_x values a decline is observed. The reason for this behavior is not clear but may

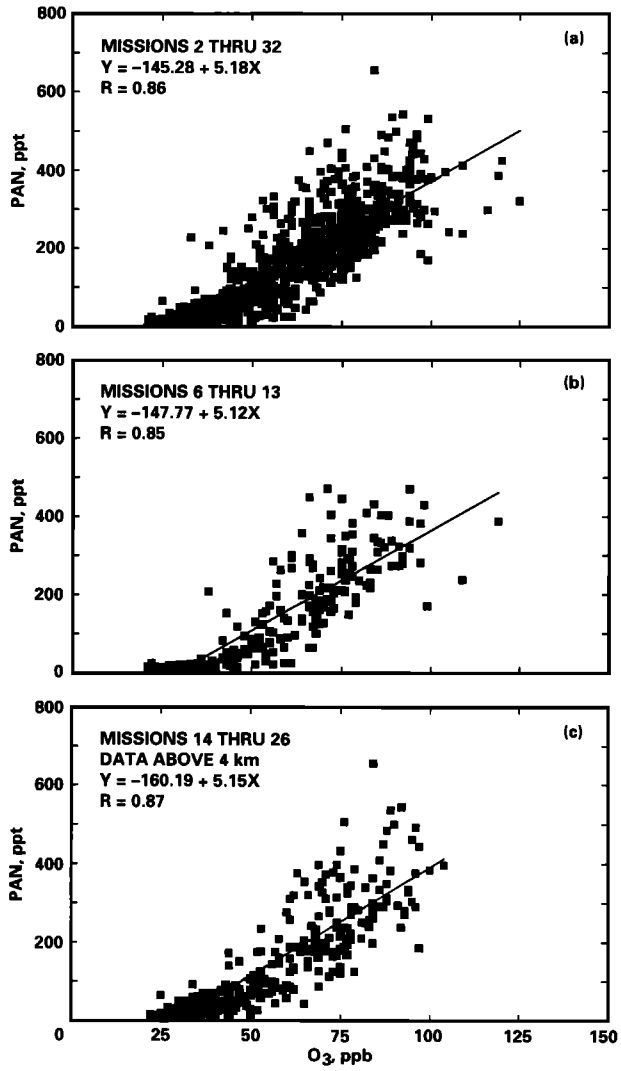

Fig. 8. Relationship between PAN and O_3 in the Arctic and sub-Arctic troposphere. Ozone data from a few instances when stratospheric intrusions may have been intersected (O_3>125 ppb) are not included in these correlations. (*a*) All data north of 50°N. (*b*, *c*) Arctic and sub-Arctic data based on flights deployed from Barrow (71°N) and Bethel (61°N), respectively.

indicate a threshold beyond which the availability of the PA radicals rather than NO_2 (PA + NO_2 → PAN) become limiting. Associated higher NO values then have the further effect of reducing PAN by acting as a sink for PA radicals (PA + NO → CH_3 + NO_2 + CO_2). It is also possible that higher NO_x values indicate recent emissions and photochemistry has not yet occurred to completion.

NO_y. Figure 10 shows that the overall PAN-NO_y relationship is similar to that of PAN-NO_x with a maximum at about 700 ppt NO_y. It should be noted that since PAN is a significant component of NO_y, a degree of autocorrelation is present. Extremely high NO_y values may indicate fresh emissions (e. g. from fires) where photochemistry has not yet produced the maximum possible PAN. It is further noted that NO_y behavior is correlated with anthropogenic tracers such as C_2H_2, CO, and C_2Cl_4 (Figure 11), suggesting that a significant impact from anthropogenic activities is present. The 3-D model calculations with the Lawrence Livermore National Laboratory (LLNL) and Geophysical Fluid Dynamics Laboratory (GFDL)

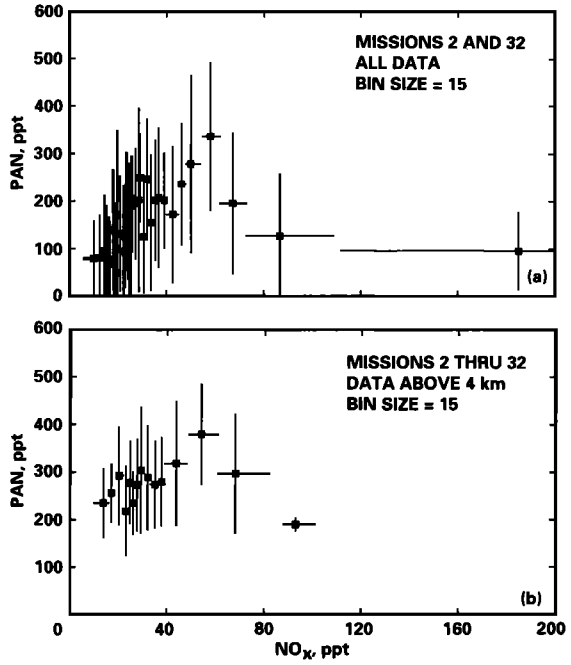

Fig. 9. Relationship between PAN and NO_x in the Arctic and sub-Arctic troposphere. As in Figure 4.

models show that at 60° to 70°N, the stratospheric contribution to tropospheric NO_y is in the 10 to 80 ppt range at 5.5 km and <1 ppt at the surface and is nearly all HNO_3 [*Levy et al*, 1980; *Kanakidou et al.*, 1991; *Kasibhatla et al.*, 1991]; (J. Penner, private communication 1991). The substantial spread in free tropospheric estimates of 10 ppt (J. Penner, private communication, 1991) and 80 ppt [Kasibhatla et al., 1991] is a measure of uncertainty in 3-D models, largely due to the difficulties in rainout/washout parameterization processes,

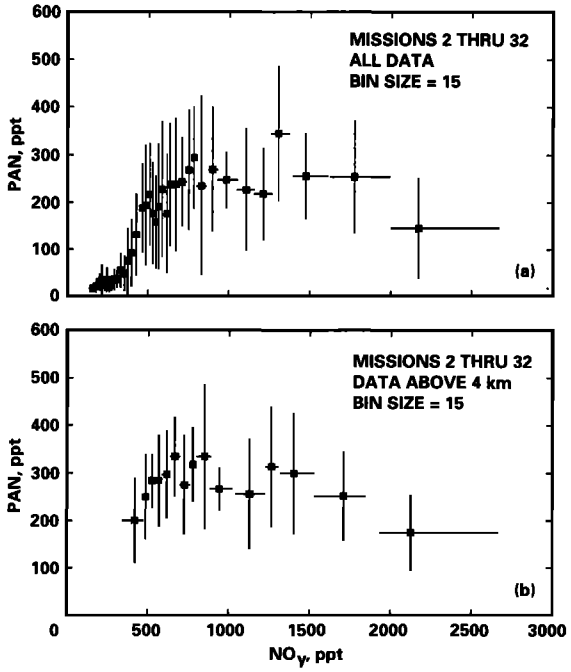

Fig. 10. Relationship between PAN and NO_y in the Arctic and sub-Arctic troposphere. As in Figure 4.

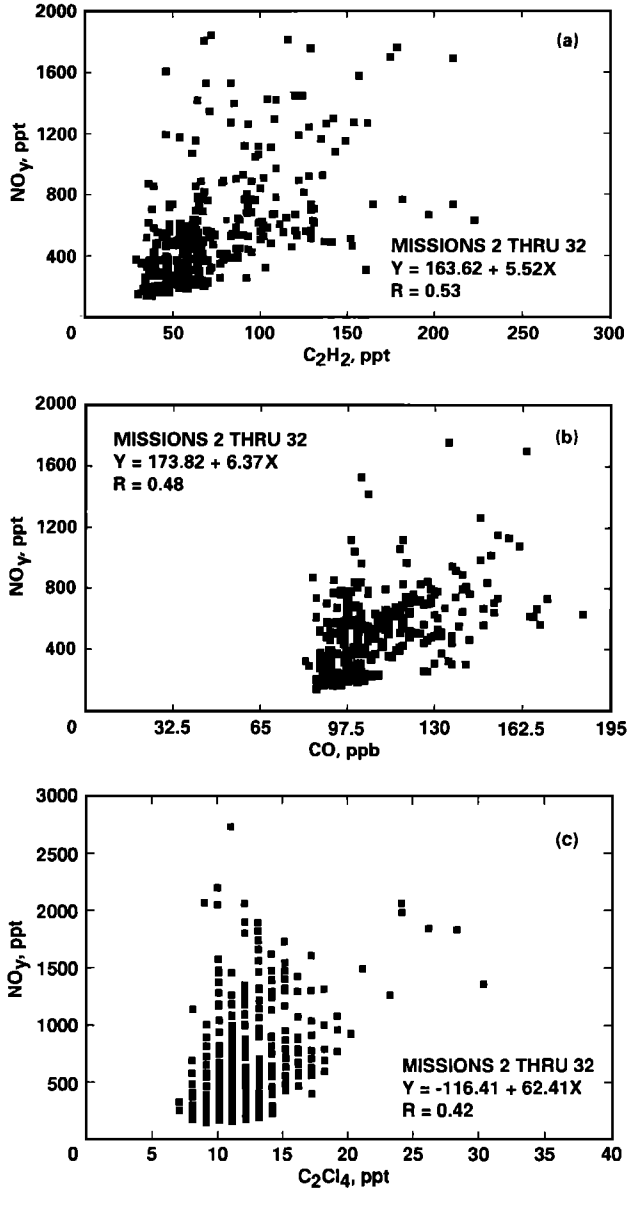

Fig. 11. Relationship between NO_y and select tracer molecules in the high-latitude (>50°N) troposphere.

especially since the amount of NO_y injected from the stratosphere is nearly identical in these models (≈1 Tg/yr). Thus at high latitudes the stratospheric contribution to summertime tropospheric NO_y is quite small. In addition, the composition of this Arctic/sub-Arctic NO_y, which is low in HNO_3 and high in PAN and possibly organic nitrates [*Singh et al.*, this issue], is completely different from that of stratospheric NO_y, which is principally HNO_3 [*Hübler et al.*, 1990; *Kondo et al.*, 1990]. These arguments support the view that the Arctic/sub-Arctic NO_y measured during ABLE 3A is predominantly of anthropogenic origin with a minor component from the stratosphere.

Tracers. Increasing PAN levels are generally associated with increasing concentrations of tracers such as C_2H_2 and CO, even though these relationships may not be linear. Figure 12 shows free tropospheric PAN-CO and PAN-C_2H_2 correlations. These relationships are similar to those for NO_y and once again point to anthropogenic impacts.

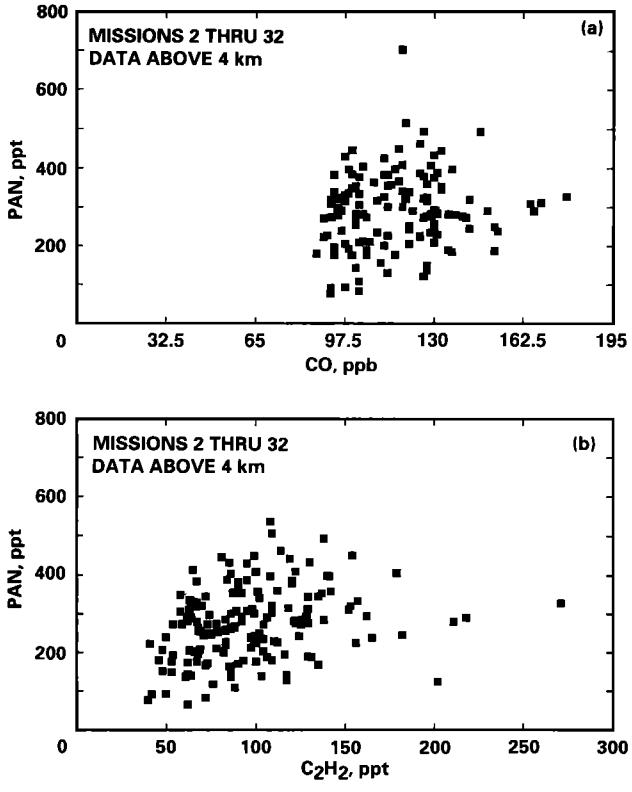

Fig. 12. Relationship between PAN and select tracer molecules in the high-latitude (>50°N) troposphere.

Overall, the relationship of PAN with other chemical parameters during ABLE 3A is consistent with findings from other latitudes in the northern hemisphere [*Singh, et al.*, 1990*a*, *b*]. The simplest association is between PAN and O_3. ABLE 3A data are consistent with the view that a substantial part of the reactive nitrogen budget at the high-latitude environments must find its original source in man-made pollution. A significant perturbation of the high-latitude troposphere is evident.

Special Case Studies

During the 33 ABLE 3A missions, a number of opportunities presented themselves to study specialized phenomenon. Here we present four cases involving stratospheric intrusions, sea and land differences, forest fires, and man-made pollution.

Stratospheric Intrusion. Stratospheric intrusions were encountered a number of times during ABLE 3A [*Browell et al.*, this issue]. One of the strongest intrusion was sampled during mission 8 (July 15/16). Figure 13 shows the PAN, O_3, NO_x, and dew point behavior during mission 8. At an altitude of about 4.4 km around 2200 UT, O_3 values reached 270 ppb (NO_y = 0.63 ppb) and the dew point temperature dropped to a low value of -41°C. NO_x and NO_y mixing ratios showed increases reflecting their stratospheric source. Tropospheric tracers such as C_2Cl_4 and C_2H_2 showed significant drops. As is evident from Figure 13, PAN levels slightly increased as the intrusion was intercepted. The O_3/NO_y ratio of about 430 measured within this intrusion is much higher than the typical tropospheric values encountered during ABLE 3A (mean O_3/NO_y =124±48 for 0-4 km and 106±50 for 4-6 km) but closer to values of 200 to 500 found in the high-latitude lower stratosphere [*Hübler et al.*, 1990; *Kondo et al.*, 1990].

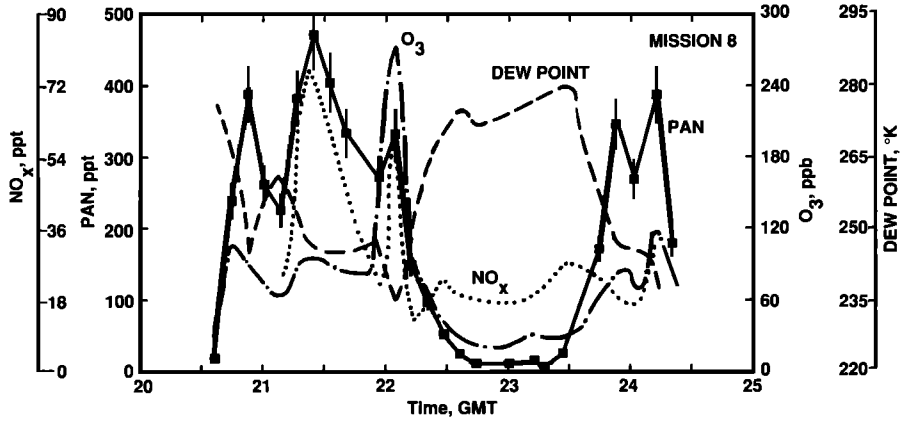

Fig. 13. PAN within a stratospheric intrusion (mission 8). Corresponding O_3, NO_x and dew point data are also shown. The aircraft remained at a constant altitude of 4.4 km from 2100 to 2225 UT. After intersecting the intrusion, it descended, reaching the 200-m level at 2270 UT.

Although no measurements from the stratosphere have been published to date, these data suggest that substantial concentrations of PAN in the upper troposphere and lower stratosphere may exist.

Ocean-land variabilities. It was repeatedly observed that in the boundary layer, PAN over land was higher than over water. Figure 14 shows one such example (mission 19, August 2/3) when the aircraft flew over water and land at about 200-m altitude. PAN levels nearly doubled when the land mass approached. A similar increase when PAN levels increased from about 12 ppt to 26 ppt was also observed during mission 17. The reasons for this rapid transition are not likely to be associated with the additional soil sources of NO_x, which are very small [*Bakwin et al.*, this issue] and indeed both NO_x and NO_y did not perceptibly change during this transition. It is also noted that in virtually all such instances the land air temperature was warmer than the marine air; hence PAN was actually less stable over land than over water. A more plausible explanation lies in the more rapid vertical mixing, caused by warmer land temperatures, with the reservoir aloft. This is further supported by the observation that O_3 was also about 2 ppb higher over land than over water.

Forest fire plumes. Figure 15 shows PAN enhancement at around 2 km inside a haze layer intersected during the overland mission 14 (July 26/27). Inside the haze layer NO, O_3, and CO showed concurrent increases. Other trace species such as C_2H_2 and C_2H_6 also showed significant excursions, while synthetic species such as C_2Cl_4 were unchanged. It is likely that this haze layer consisted of residual smoke from forest fires that had been burning in the area during the previous several days [*Drewery*, 1988]. Within the plume a significant fraction of NO_x had been converted to PAN. Forest fire plumes and their chemistry have been further studied by *Wofsy et al.* [this issue] and *Jacob et al.* [this issue].

North Pacific pollution episode. During the Cold Bay (Aleutian Islands) flight of mission 23 (August 7/8) a pollution episode was observed within the free troposphere over the North Pacific Ocean. PAN, O_3, NO_y, C_2Cl_4 vertical profiles (Figure 16) show significant disturbance in the 4 to 6 km

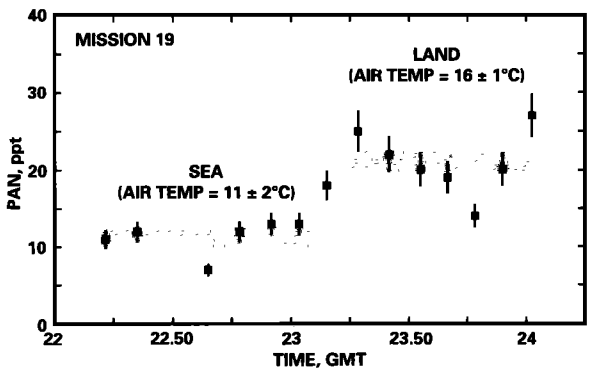

Fig. 14. PAN at the sea-land interface in the sub-Arctic boundary layer (mission 19). The aircraft remained at a constant 150-m altitude.

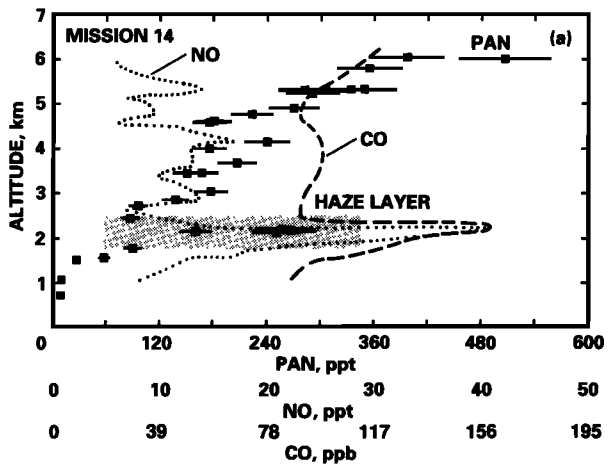

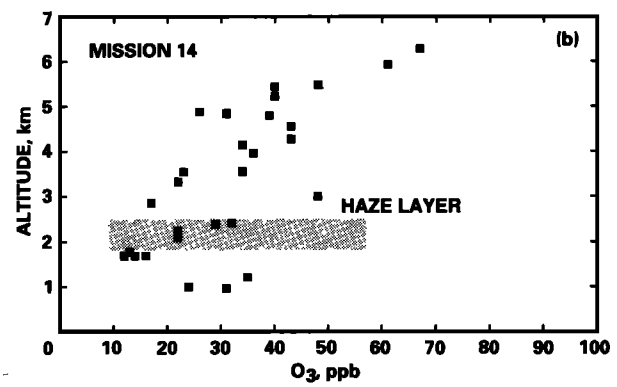

Fig. 15. PAN, NO, O_3, and CO within a plume impacted by forest fires (mission 14). Shaded area shows the haze layer as seen by the UV lidar.

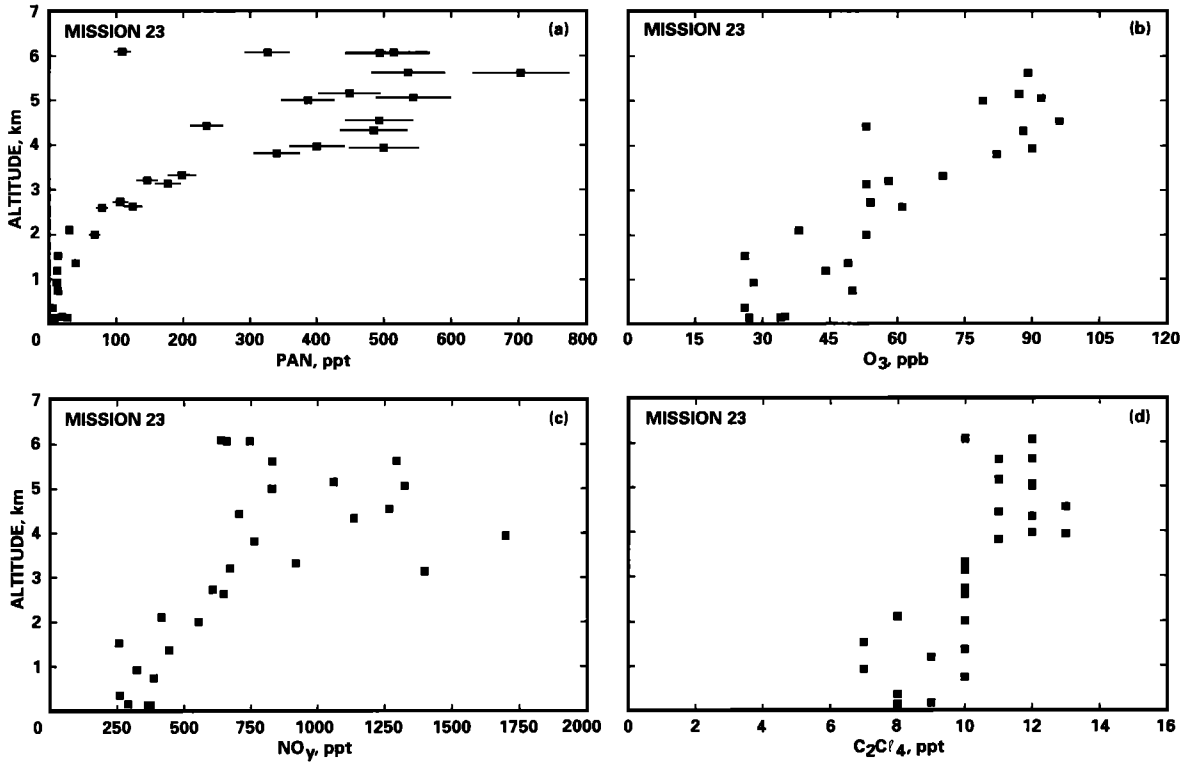

Fig. 16. High-altitude pollution episode over the North Pacific Ocean (mission 23).

region. The upper level enhancement and variability could also be seen in the vertical structures of CO, C_2H_2, C_2H_6, and radon. The high C_2Cl_4 levels provide a distinct signature of man-made pollution. Trajectory analyses suggest that this upper tropospheric air mass may have been impacted by pollution from eastern Siberia [*Drewery*, 1988].

Conclusions

The ABLE 3A field study has shown that large concentrations of PAN and NO_y are present in the Arctic/sub-Arctic troposphere of the northern hemisphere during the summer. Mixing ratios of PAN as well as a variety of other molecules are more abundant in the free troposphere compared to the boundary layer. Coincident PAN and O_3 atmospheric structures suggest that phenomena that define PAN also define the corresponding O_3 behavior. Unlike the lower stratosphere, where NO_y is mostly made up of HNO_3, tropospheric Arctic/sub-Arctic NO_y has little HNO_3. Model calculations, correlations between NO_y and anthropogenic tracers, and the composition of NO_y itself suggest that the Arctic/sub-Arctic reactive nitrogen measured during ABLE 3A is predominantly of anthropogenic origin with a minor component from the stratosphere. It is possible that high levels of pollution transported from industrial regions, with significant NMHC and NO_x loading, are trapped in the stable Arctic atmosphere in winter and early spring and this charged reservoir photochemically generates significant quantities of PAN as summer approaches. Superimposed on this anthropogenically polluted reservoir are natural forest fire plumes and air of stratospheric origin. This view implies that important concentrations of simple and complex organic nitrates may also be present in the Arctic/sub-Arctic atmosphere. It is suggested that the tropospheric PAN (and NO_y) reservoir could be an important contributor to the summertime maximum in deposited nitrate observed over Greenland. Studies extending over several seasons, especially the spring-summer transition, are needed to fully understand the perturbations to the high-latitude troposphere.

Acknowledgments. This research was supported by the NASA Global Tropospheric Experiment. We acknowledge all ABLE 3A participants for their cooperation and support. Special thanks are due to the flight and ground crew of the Wallops Electra for making this effort a success. We greatly appreciate the computational assistance provided by D. Dempsey and B. Sitton of the Synemet Corporation.

References

Atkinson, R., Gas-phase tropospheric chemistry of organic compounds: A review, *Atmos. Environ., 24A*, 1-41, 1990.

Bakwin, P. S., S. C. Wofsy, and D. R. Fitzjarrald, Measurements of NO_x and NO_y concentrations and fluxes over Arctic tundra, *J. Geophys. Res.*, this issue.

Barrie, L. A., Arctic air pollution: An overview of current knowledge, *Atmos. Environ., 20*, 643-663, 1986.

Blake, D. R., D. F. Hurst, T. W. Smith, Jr., W. J. Shipple, T. Y. Chen, N. J. Blake, and F. S. Rowland, Summertime measurements of selected nonmethane hydrocarbons in the Arctic and sub-Arctic during the 1988 Arctic Boundary Layer Expedition (ABLE 3A), *J. Geophys. Res.*, this issue.

Bottenheim, J. W. and A. G. Gallant, PAN over the Arctic: Observations during AGASP-2 in April 1986, *J. Atmos. Chem., 9*, 301-316, 1989.

Browell, E. V., C. F. Butler, S. A. Kooi, M. A. Fenn, R. C. Harriss, and G. L. Gregory, Large-scale variability of ozone and aerosols in summertime Arctic and sub-Arctic troposphere, *J. Geophys. Res.*, this issue.

Calvert, J. G., and S. Madronich, Theoretical study of the initial products of atmospheric oxidation of hydrocarbons, *J. Geophys. Res., 92*, 2211-2220, 1987.

Crutzen, P. J., The role of NO and NO_2 in the chemistry of the troposphere and stratosphere, *Annu. Rev. Earth Planet Sci.*, 7, 443-472, 1979.

Davidson, C. I., J. R. Harrington, M. J. Stephenson, M. J. Small, F. P. Boscoe, and R. E. Gandley, Seasonal variations in sulfate, nitrate and chloride in the Greenland Ice Sheet: Relation to atmospheric concentrations, *Atmos. Environ., 23*, 2483-2494, 1989.

Drewery, J. W., GTE/ABLE 3A aircraft meteorological and navigational data including met synopses, Expedition flights 1–33, July 7 to August 1988.

Fehsenfeld, F., C. et al., A ground based intercomparison of NO, NO_x, and NO_y measurement techniques, *J. Geophys. Res.,92*, 14,710-14,722, 1987.

Haagen-Smit, A. J., Chemistry and physiology of Los Angeles smog, *Ind. Eng. Chem., 44*, 1342-1346, 1952.

Harriss, R., et al., The Arctic Boundary Layer Expedition (ABLE 3A): July–August 1988, *J. Geophys. Res.*, this issue.

Hov, O., S. A. Penkett, I. S. A. Isaksen, and A. Semb, Organic gases in the Norwegian arctic, *Geophys. Res. Lett., 11*, 425-428, 1984.

Hübler, G., et al., Redistribution of reactive odd nitrogen in the lower stratosphere, *Geophys. Res. Lett., 17*, 453-456, 1990.

Isaksen, I. S. A., and O. Hov, Calculation of trends in tropospheric concentrations of O_3, OH, CO, CH_4, and NO_x, *Tellus, 39*, 271-285, 1987.

Jacob D., et al., Summertime photochemistry of the troposphere at high northern latitudes, *J. Geophys. Res.*, this issue.

Joos L.F., W.F. Landolt, and H. Leuenberger, Calibration of peroxyacetyl nitrate measurements with an NO_x analyzer, *Environ. Sci. Technol., 20*, 1269-1273, 1986.

Kanakidou, M., H. B. Singh, K. M. Valentin, and P. J. Crutzen, A two-dimensional study of ethane and propane oxidation in the troposphere, *J. Geophys. Res., 96*, 15,395 to 15,413, 1991.

Kasibhatla, P. S., H. Levy II, W. J. Moxim, and W. L. Chameides, The relative impact of stratospheric photochemical production on tropospheric NO_y levels: A model study, *J. Geophys. Res., 96*, 18,631–18,646, 1991.

Kasting, J. F., and H. B. Singh, Nonmethane hydrocarbons in the troposphere: Impact on odd hydrogen and odd nitrogen chemistry, *J. Geophys. Res., 91*, 13,239-13,256, 1986.

Kondo, Y., et al., Balloon-borne measurements of total reactive nitrogen, nitric acid, and aerosol in the cold arctic stratosphere, *Geophys. Res. Lett., 17*, 437-440, 1990.

Levy, H., II, Normal atmosphere: Large radical and formaldehyde mixing ratios predicted, *Science, 173*, 141-143, 1971.

Levy, H., II, and W. J. Moxim, Simulated global deposition of reactive nitrogen emitted by fossil fuel combustion, *Tellus, 41B*, 256-271, 1989.

Levy, H., II, J. D. Mahlman, and W. J. Moxim, A stratospheric source of reactive nitrogen in the unpolluted troposphere, *Geophys. Res. Lett., 7*, 441-444, 1980.

Lillian, D., and H. B. Singh, Absolute determination of atmospheric halocarbons by gas phase coulometery, *Anal. Chem., 46*, 1060-1063, 1974.

McNeal, R. J., J. P. Mugler, Jr., R. C. Harriss, and J. M. Hoell, Jr., NASA Global Tropospheric Experiment, *Eos Trans. AGU, 64*, 561-562, 1983.

Logan, J. A., M. J. Prather, S. C. Wofsy, and M. B. McElroy, Tropospheric chemistry: A global perspective, *J. Geophys. Res., 86*, 7210-7254,1981.

Penkett, S. A., and K. A. Brice, The spring maximum in photooxidants in the northern hemisphere troposphere, *Nature, 319*, 655-657, 1986.

Penner, J., C. S. Atherton, J. J. Walton, and S. Hameed, The global cycle of reactive nitrogen, *Rep. UCRL-JC-104052*, Lawrence Livermore Nat'l Lab., Livermore, Calif., 1990.

Rahn, K. A., Progress in arctic air chemistry, 1980-1984, *Atmos. Environ., 19*, 1987–1994, 1985.

Rasmussen, R. A., M. A. K. Khalil, and R. J. Fox, Altitude and temporal variations of hydrocarbons and other gaseous tracers of Arctic haze, *Geophys. Res. Lett., 10*, 144-147, 1983.

Rudolph, J., B. Vierkorn-Rudolph, and F. X. Meixner, Large-scale distribution of PAN results from the STRATOZ III flights, *J. Geophys. Res., 92*, 6653-6661, 1987.

Sandholm, S. T., et al., Summertime tropospheric observations related to N_xO_y distribution and partitioning over Alaska: ABLE 3A, *J. Geophys. Res.*, this issue.

Schnell, R. C., Arctic haze and the Arctic gas and aerosol sampling program (AGASP), *Geophys. Res. Lett., 11*, 361-364, 1984.

Shipham, M. C. and S. A. Bachmeier, D. A. Cahoon, Jr., and E. V. Browell, Meteorological overview of the Arctic Boundary Layer Expedition (ABLE 3A) flight series, *J. Geophys. Res.*, this issue.

Singh, H. B., Reactive nitrogen in the troposphere, *Environ. Sci. Technol., 21*, 320-327, 1987.

Singh, H. B., and P. L. Hanst, Peroxyacetyl nitrate (PAN) in the unpolluted atmosphere: An important reservoir for nitrogen oxides, *Geophys. Res. Lett., 8*, 941-944, 1981.

Singh, H. B., and L. J. Salas, Methodology for the analysis of peroxyacetyl nitrate (PAN) in the unpolluted atmosphere, *Atmos. Environ., 17*, 1507-1516, 1983.

Singh, H. B., L. J. Salas, and W. Viezee, The global distribution of peroxyacetyl nitrate, *Nature, 321*, 588-591, 1986.

Singh, H., et al., Peroxyacetyl nitrate measurements during CITE 2: Atmospheric distribution and precursor relationships, *J. Geophys. Res., 95*, 10,163-10,178, 1990*a*.

Singh, H. B., et al., Atmospheric PAN measurements over the Brazilian Amazon Basin during the wet season: Relationships with nitrogen oxides and ozone, *J. Geophys. Res., 95*, 16,945-16,954,1990*b*.

Singh, H. B., et al., Relationship of Peroxyacetyl nitrate to active and total odd nitrogen at northern high latitudes: Influence of reservoir species on NO_x and O_3, *J. Geophys. Res.*, this issue.

Talbot, R. W., A. S. Vijgen, and R. C. Harriss, Soluble species in the Arctic summer troposphere: Acidic gases, aerosols, and precipitation, *J. Geophys. Res.*, this issue.

Wofsy, S. C., et al., Atmospheric chemistry in the Arctic and sub-Arctic: Influence of natural fires, industrial emmissions, and stratospheric inputs, *J. Geophys. Res.*, this issue.

D. R. Blake, University of California, Irvine, CA 92717.

J. D. Bradshaw and S. T. Sandholm, Georgia Institute of Technology, Atlanta, GA 30332.

P. J. Crutzen and M. A. Kanakidou, Max-Planck-Institüt für Chemie, D 6500 Mainz, Germany.

G. L. Gregory and G. W. Sachse, NASA Langley Research Center, Hampton, VA 23665.

D. Herlth, and H. B. Singh, NASA Ames Research Center, Moffett Field, CA 94035.

D. O'Hara, San Jose State University Foundation, Moffett Field, CA 94035.

(Received June 12, 1990;
revised March 18, 1991;
accepted March 18, 1991.)